CHALLENGES IN THE DESIGN OF RADIAL TURBINES FOR SMALL GASOLINE ENGINES

Graham Cox

PCA Engineers Limited, Lincoln, UK

E-mail address: graham.cox@pcaeng.co.uk

Abstract

The modern trends in automotive turbocharger applications are towards the boosting of smaller internal combustion engines in passenger cars. The use of turbochargers in gasoline engines is increasingly common.

There are particular issues relating to gasoline engines that result in the aerodynamic efficiency of the turbine design being less than the achievable. The turbine must be designed to provide the best compromise between engine efficiency and transient response. This paper explains the reasons for compromise in the design and presents an example of a design methodology by which a design optimum may be developed.

1. Introduction

Turbocharger turbines, especially those for passenger car engines, are not generally designed to be as efficient as possible. They are designed to provide the best compromise between engine efficiency and transient response and to support a compact turbocharger package. The shaft speed is typically selected to suit the compressor and tends to be higher than would be chosen by the turbine designer were good aerodynamic efficiency to be the predominant requirement. The optimum design can only be demonstrated at system level, so the turbine designer's goal is usually to provide the "best" turbine to suit the system requirements.

After explaining the compromise placed on the aerodynamic design of the turbine, the paper goes on to describe a method, by which candidate wheels can be developed that are optima within the geometric constraints. The described optimisation method uses 2D (throughflow) for assessment of aerodynamic performance. 3D CFD is assumed to provide the best indicator of relative performance of candidate wheel designs. The paper includes comparisons between 2D and 3D CFD analyses of designs in a typical study.

Beyond the development of the wheel design 3D CFD is also used to support other features of the turbine stage. Examples are given to present a more complete picture of how the design challenges may be addressed ahead of prototype manufacture.

2. The compromised turbine design

The turbine designer would like to select an optimum speed to suit a set of design point boundary conditions. These would usually be those appropriate to low engine speed where high torque is required at low engine flow for good transient response.

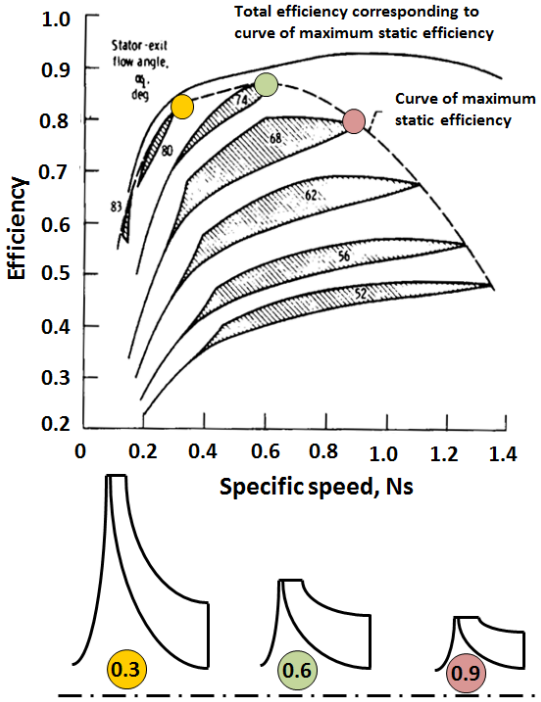

Figure 1: The effect of specific speed on achievable efficiency according to Rohlik [1]

The optimum aerodynamic speed is typically chosen based on specific speed, Ns, where:

$$Ns = \frac{\omega Q_2^{0.5}}{\Delta h_{0S}^{0.75}} \qquad (1)$$

For a turbocharger turbine, where there is no opportunity for downstream static pressure recovery, attention is focussed on total-static efficiency, $\eta_{T\text{-}S}$. The empirical observations of Rohlik [1], presented in Figure 1, suggest that the ideal specific speed is approximately 0.6. The aforementioned requirements of compressor design and a compact package tend to lead to a turbine specific speed closer to 0.8. It is evident from the $\eta_{T\text{-}S}$ curve in Figure 1 that this results in a significant penalty in achievable efficiency. The physical explanation for this is evident

from the representative turbine wheel schematics at the bottom of Figure 1. The high speed wheel is of relatively low diameter so the exducer area is low and the exit gas velocity is high. A high exit kinetic energy represents wasted energy.

The design is then further compromised, in an efficiency sense, by minimising the inertia of the turbine wheel. The turbine wheel is the major source of inertia in the turbocharger rotor, and its reduction has a first order effect on rotor acceleration. Figure 2 shows how this is done: by reducing the outer radius, R_1. The exducer radius, R_2 is kept as high as possible to minimise the exit dynamic head. The dashed line of the reduced inertia variant shows the most extreme inertia reduction. The "cut-back" leading edge design is sometimes referred to as a "mixed-flow" turbine.

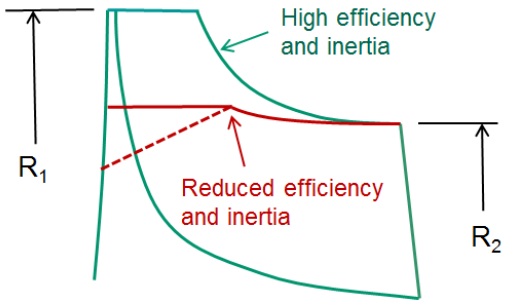

Figure 2: How inertia is reduced in a turbine wheel

That this inertia reduction strategy adversely affects efficiency is evident from another classic empirical chart, that of Rodgers & Geiser [2]. Figure 3 shows that the highest achievable efficiency occurs when the Blade-Speed-Ratio, U/C, is close to 0.7.

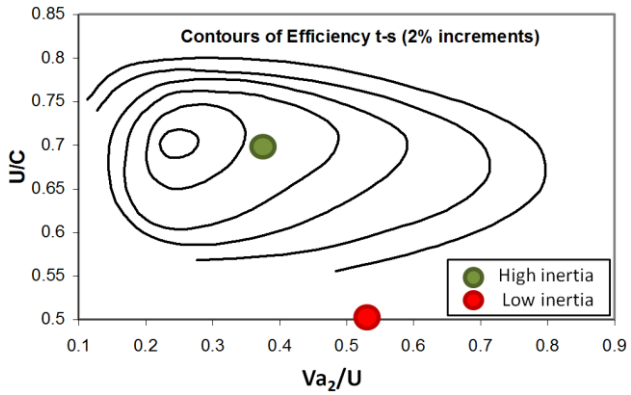

Figure 3: Effect of inertia reduction on efficiency

U is the blade tip velocity at R_1 and C is the spouting velocity (see Nomenclature). The optimum value is found where the wheel experiences the maximum gas acceleration in the rotor passage and minimum exit kinetic energy. The green and red points placed on Figure 3 represent high and low outer radius designs having constant Ns of about 0.8. The outer radius of the low inertia design is represented as a ratio of 5:7 of the high inertia design, resulting in a direct reduction in U/C. Assuming identical exducer flow area, the flow coefficient, Va_2/U, increases in inverse proportion. For constant exducer area, the U/C reduction is the dominant cause of efficiency reduction. If the designer aims to minimise exit kinetic energy the tangential component of the exit flow must be close to zero in the absolute sense. This implies a high relative inlet swirl angle resulting in high blade incidence and poor flow acceleration in the rotor passage as shown in Figure 4. An alternative strategy is to increase reaction, i.e. increase rotor passage acceleration and absolute exit swirl. This has not been found to be aerodynamically superior in general and leads to the requirement for a larger turbine inlet scroll and causes an increase in the turbine wheel metal temperature.

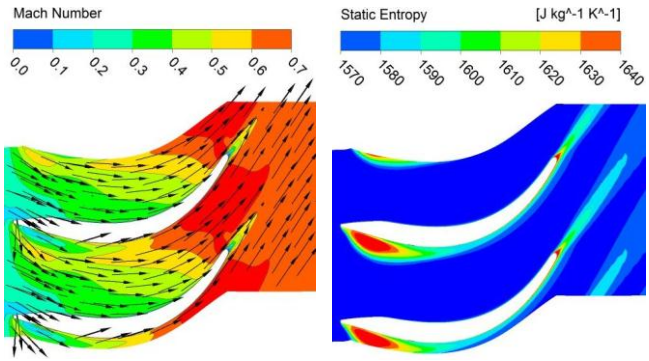

Figure 4: Leading edge separation evident in low U/C operation (CFD calculation)

This description presents the major physical issues that constrain the turbine designer, but even after R_1 is defined (approximately) there is still great scope to vary the vane geometry, and thereby develop the best design. By varying, for example, axial length, number of vanes, and the hub profile, a large number of mechanically acceptable potential designs may be produced. These can be displayed on a plot of $\eta_{T\text{-}S}$, according to CFD calculation, against the inertia, as shown in Figure 5.

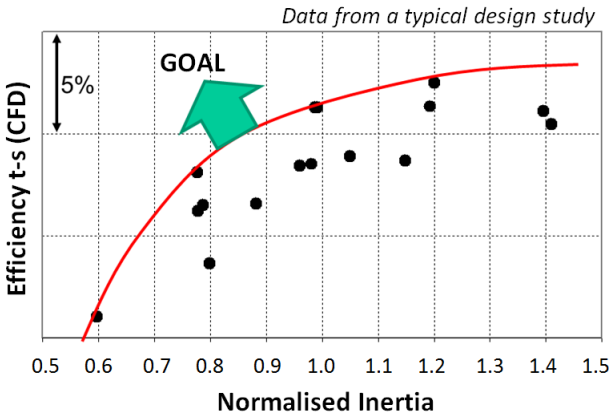

Figure 5: Pareto front of best designs from a design study

It is the job of the system designer to identify which design best satisfies the overall requirement of the engine plus turbocharger system. It is the aim of the turbine designer to push the Pareto front in the direction of the

arrow in Figure 5. For the turbine wheel there are three ways by which this can be achieved:

- Selection of superior, creep resistant materials.
- Minimising mechanical design margins through analysis and test.
- Better, integrated, aerodynamic/structural design.

The first and second items are outside the scope of this paper. The subsequent section of this paper describes one integrated methodology that supports better design with the potential for continuous improvement.

It is worth noting, also, that there are issues of thermal management and bearing loss that will be affected by the turbine design. These are not included in the following description of design methodology, but could be included where empirical knowledge is available.

3. Design methodology

The turbine experiences a large range of operating conditions associated with the pulsatile nature of the flow exiting the engine exhaust ports. For practical purposes it is necessary to have a single design point, which is usually taken as the average conditions over the pulse that is of most interest to the system designer, typically low engine speed and full power. For reasons explained in the previous section the turbine wheel diameter is set such that the design point U/C is in the range of 0.50 to 0.55. It is common also to consider the conditions experienced by the turbine at pulse peak since a high fraction of power is absorbed close to this point. U/C tends to be in the range of 0.30 to 0.35 at this condition. This represents an extreme aerodynamic condition and not one that is considered appropriate for design. It is more appropriate to consider it as an analysis point for helping establish the best designs.

3.1. Basic principles of design

The basic relationship in design is that between geometry and performance prediction, where the performance is both aerodynamic and structural. For aerodynamic optimisation, the geometry definition will be limited by the capability of the performance prediction method to discriminate between changes in the geometric parameters (at least in a qualitative sense).

At the simplest level empiricism of the form shown in Figures 1 and 3 can be used to trade-off overall size, speed and efficiency. More useful 1D empirical design models are available, for example those described by Whitfield and Baines [3] and Suhrmann et. al. [4]. These allow a small level of optimisation, e.g. in number and length of vanes and the inlet and exit velocity triangles. About 12 geometric parameters are enough to define a simple radial turbine. Good 1D empiricism allows changes in many (but not all) to indicate expected performance change. In state-of-the-art design this is inadequate to investigate the subtle design changes that can significantly improve performance.

It is necessary to move up to methods employing physics-based fluids solvers to support the investigation of these subtle design changes. The most accurate method is 3D, Navier-Stokes CFD. With 30 to 50 geometric parameters it is possible to generate advanced turbine vane geometry and the effects of changing any of these on aerodynamic efficiency can be predicted with reasonable confidence. Figure 6 indicates that a combination of meridional passage, vane angle and thickness definition are translated into 3D geometry for hi-fidelity analysis.

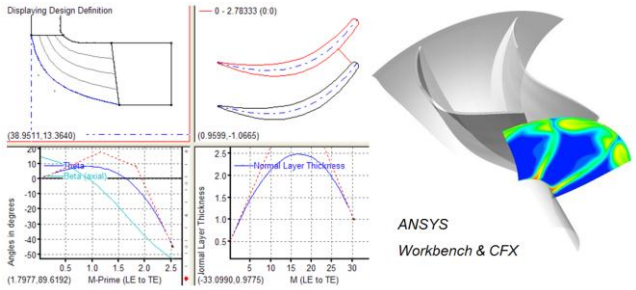

Figure 6: Inputs and output from 3D design / analysis

An experienced designer can develop an efficient design, but the permutations of the parameters are too large to ensure that an optimum design has emerged. The process of testing parameter combinations automatically and training the system to improve designs is becoming more established but it is still extremely time consuming to develop an optimum design. In the long-term, as computer power continues to increase, it is anticipated that the solution time for a rigorous optimisation will fit within the standard routine design cycle time.

A pragmatic alternative is to solve the fluid equations as applied to the circumferentially averaged, meridional flow field using streamline curvature equations (throughflow). Despite being a 2D analysis, the same 3D geometry is used for establishing the equations that account for gas-turning and aerodynamic blockage. Figure 7 shows that the predicted velocity field can be quite similar. 2D is not guaranteed to be as good at reproducing the meridionally averaged 3D flow as shown in Figure 7, as will be discussed in a later section.

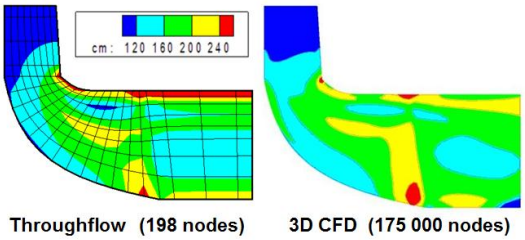

Figure 7: Meridional velocity from 2D and 3D CFD

Throughflow is an established and still important method used in axial turbine design [5] to ensure the integrity of the flow field before performing profile design. It reveals many key flow features before 3D analysis is required.

Because it supports the development of 3D geometry and it is very quick to solve it is ideally suited to an optimisation process. This reads across to the design of radial turbines.

Whether 2D or 3D aerodynamic analysis is used, there is a common strategy to the optimisation of a design (or designs). A group of rival variants is produced. Each comprises a set of geometry parameters that can be read into automatic meshing tools for submission to 2D or 3D CFD analysis. In the case of 3D analysis, the aerodynamic performance outcomes are used directly. In the case of 2D analysis, features of the flow-field are converted into aerodynamic fitness values that, together, can be treated as a proxy for efficiency. In both cases, candidate designs that pass the aerodynamic acceptability test are submitted to structural assessment. Those that pass this test go on to influence a new generation of designs following an appropriate evolutionary strategy.

3.1.1. 3D strengths and weaknesses

The 3D CFD prediction of aerodynamic performance, i.e. the efficiency and the mass-flow at the design expansion ratio (or exit pressure at the design mass-flow), is the best available from numerical methods. However, even with modern computers and a fairly coarse computation mesh, the run-time for a single geometry will be a number of minutes, so it is difficult to explore a significant design space in an acceptable time. It is expected that this situation will improve as the "intelligence" of the design system is improved.

3.1.2. 2D strengths and weaknesses

A throughflow calculation can be carried out within a few seconds so 1000s of geometries can be considered quickly. However, the ability to evolve optimum designs is dependent on the reliability of the aerodynamic fitness calculation. This is not always reliable, so it is necessary to submit a number of candidates to subsequent 3D analysis to minimise the chance that good designs are ignored. The system is improved if, at the end of a design exercise, the aerodynamic fitness routine is reviewed to ensure that good and bad designs are ranked accordingly.

3.2. 2D optimisation

Results presented in Section 4 were generated using an optimisation method that has been reported elsewhere [6, 7]. A summary is provided here to give greater appreciation of the following results.

The parameters that go into the optimisation process are dimensions normalised to R_1 and blade angles, see Figure 8. Curves are constructed using parameterised Bezier points. It is usually assumed that the vane is radially stacked and that the tip thickness is known. This leaves a balance of typically 30 variable parameters. The parameters are processed to generate an "RTZT" format file for input to the throughflow code [8].

The throughflow code requires loss and deviation models to generate a representative flow-field. The deviation model [9] takes account of both the trailing edge angle and the cosine rule angle with a treatment to allow for the under-turning associated with over-tip leakage and the main passage vortex. Loss is distributed in a physically representative manner, i.e. biased towards the casing with a peak at 88% span with a magnification factor of three. This is considered generally realistic for turbocharger turbine studies. It is important to note that it is not necessary for the throughflow code to make a prediction of the quantity of loss. It is sufficient that the combination of passage geometry, deviation and loss distribution leads to a good simulation of the meridional flow fields, as exemplified by Figure 7.

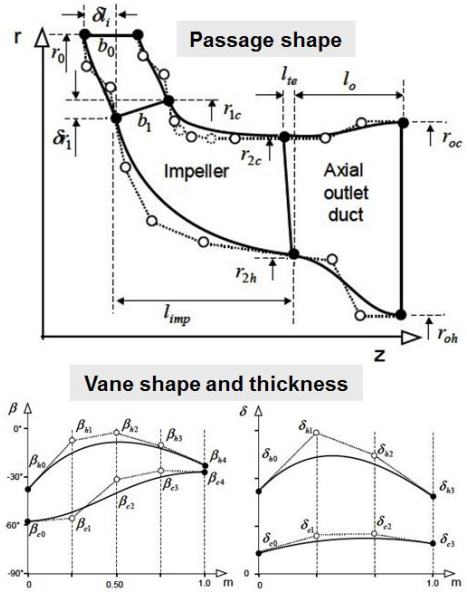

Figure 8: Geometry parameters

Following the throughflow calculation on a candidate geometry an aerodynamic penalty function is calculated as the sum of individual penalties on a range of fitness parameters, extracted from the throughflow solution, as listed in Table 1.

Table 1: Contributors to the aerodynamic penalty function

Aerodynamic fitness parameter	Relative weighting
Work coefficient *De Haller number (W_2/W_1)*	*High*
Profile loss ($\propto W^3$) *Maximum blade loading* *Acceleration linearity on mean streamline* *Peak diffusion on the casing streamline*	*Medium*
Casing leading edge incidence *Hub leading edge incidence* *Exit flow coefficient (axial)* *Exit flow coefficient (circumferential)* *Trailing edge diffusion at the hub*	*Low*

The selection is based on experience of features that a designer would expect to consider in improving a design. Of particular note is the work coefficient. Deviation from the target value is penalised highly to eliminate designs that do not meet the fundamental work requirement. The weightings of the other parameters have been developed so that the overall penalty correlated with CFD analysis carried out on the same geometry. The performance of the current set of weightings is shown in Figure 9. Additional penalty functions are provided for hub throat width, which is often a serious constraint on designs, and inertia, to provide a potential forcing mechanism to help develop low inertia designs.

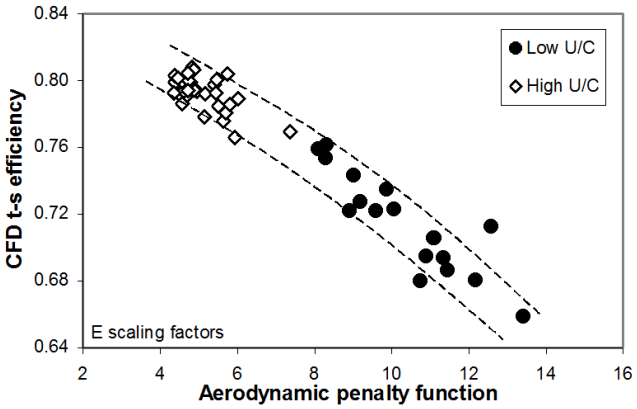

Figure 9: Sample correlation between CFD efficiency and optimiser aerodynamic penalty function for the same geometries

As the optimisation process progresses, potential designs that meet an aerodynamic acceptance criterion are submitted to a basic finite element structural analysis on a single, rigidly hub-constrained vane. The test conditions, and the limits applied to the study in Section 4 are recorded in Table 2. The calculations are carried out at 130% of aerodynamic design speed and the metal temperature is assumed to be a weighted average of the inlet and exit total temperature, specifically 30% of the inlet and 70% of the exit value. It is standard practice to ignore the candidate designs that have failed to meet any of the structural targets.

Table 2: Applied structural test conditions

Structural test conditions	Limit
Peak vanes stress	*1.5 safety margin*
Creep Life	*100 hours*
1st flap modal frequency	*4/rev +10%*

The optimisation process involves submitting a population of, typically, 60 designs within an initially specified range of geometric parameters to 2D aerodynamic analysis. As stated above, acceptable designs are then submitted to structural checking. On subsequent generations new designs are developed from the old by adding a random parameter vector to each one. The aerodynamic fitness is assessed and a superior design will replace its predecessor. Designs that are better combinations of aerodynamic fitness, structural score and inertia are saved. The build-up of progressively better designs forms a Pareto front that allows the designer to pick a small sample of designs for more rigorous analysis. Experience has demonstrated that it is best to run a series of cases of small population and small parameter ranges. The parameter ranges are modified for each run, if necessary, to avoid the ranges constraining the development of design optima.

4. Results from an optimisation study

The optimisation study described in detail in [7] included a low U/C case having key non-dimensional, design point aerodynamic and geometric parameters that are typical of modern gasoline engine turbocharger turbine. They are recorded in Table 3.

Table 3: Non-dimensional features for study

U/C	0.50
Va_2/U	0.55
Ns	0.78
Expansion ratio t-s	2.03
Tip Mach number	0.50
Vane tip thickness *	1%
Tip clearance *	1%
Minimum throat width *	4%
** % of tip diameter*	

The optimisation process was applied to this case resulting in a range of structurally acceptable designs that presented a Pareto front of 9-vane designs, as shown in Figure 10. The data comprise 13 individual optimisation runs to ensure coverage over the full region of interest.

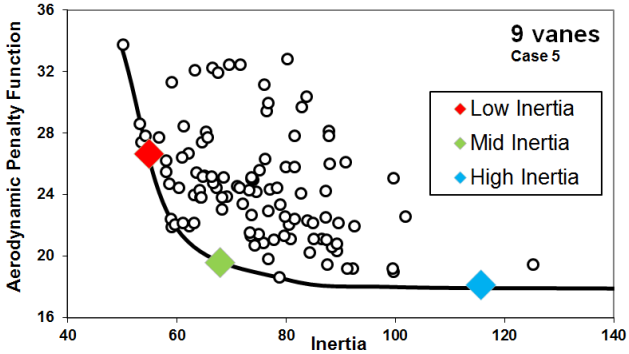

Figure 10: Optimiser Pareto front established for a low U/C turbine

The designer is most likely to be interested in designs on the Pareto front. Three are identified for more rigorous analysis, identified as: Low Inertia, Mid Inertia and High Inertia. Inspection of the designs is the first step: do they display obvious geometric weaknesses that make the 2D aerodynamic assessment suspect? Are the vane shapes too extreme for manufacture? Is there a reasonable geometry trend linking the Pareto front designs? Figure 11 compares the meridional and blade-to-blade shapes of

the three selected designs. The geometry trends are consistent: higher inertia is associated with greater length, higher exducer radius and lower pitch/chord ratio for the vane. In all cases the passage contraction is good. The low inertia design has a more cut-back leading edge. All are considered suitable for 3D CFD analysis.

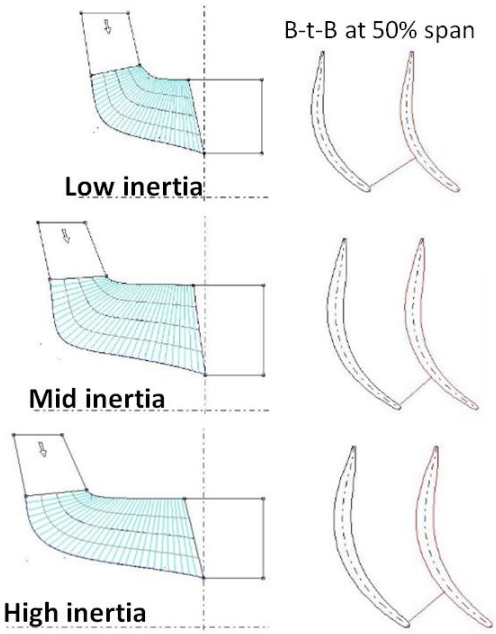

Figure 11: Selected designs from the Pareto front

4.1. CFD analysis and comparison

CFD analysis for comparison purposes requires systematic meshing, set-up and post-processing to ensure that results from rival geometries compare fairly. At this stage the turbine wheel is considered in isolation. A typical set-up is shown in Figure 12. Other standards are:

- Typical mesh size: 150k nodes
- Y+ <10 on rotor walls
- SST (RANS) turbulence model
- Ideal gas treatment

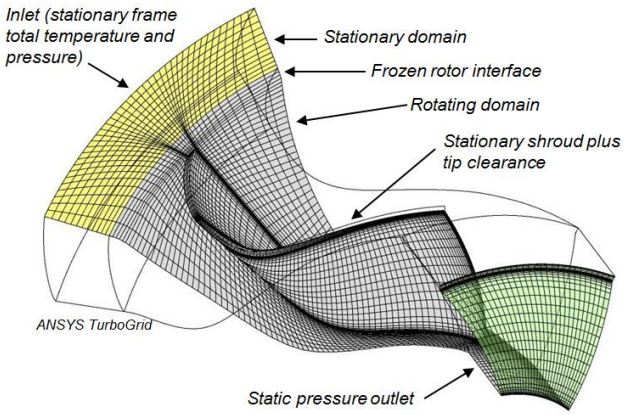

Figure 12: CFD model set-up

The inlet stagnation conditions and t-s expansion ratio are defined so mass flow will be an output of the CFD analysis. It is necessary to adjust the inlet swirl angle until the target mass-flow is achieved. This has been done for the three selected designs as shown in Figure 13. At the target mass-flow, i.e. that specified for the optimisation, the efficiency is much lower for the Low inertia design. The efficiency of the High inertia design is slightly higher than that of the Mid inertia design. This ranking is in line with the aerodynamic penalty functions shown in Figure 10. It is interesting to note the much lower inlet swirl angle for the Low inertia design. This implies a larger scroll A/R, which is not so good for package size.

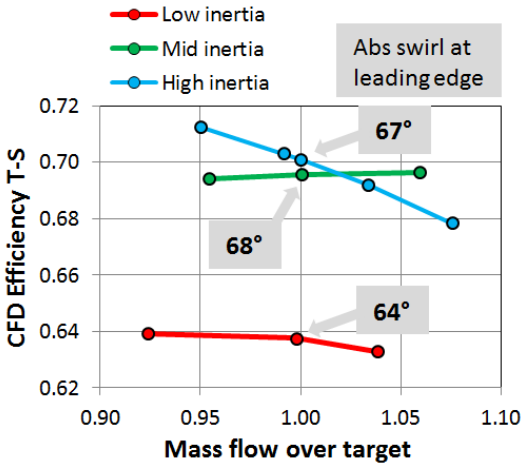

Figure 13: Establishing design point performance using CFD

For understanding the limits of the 2D aerodynamics based optimisation method it is necessary to compare the 2D and 3D CFD predictions. Figures 14 to 16 present the meridional plots of two velocity components at the target mass-flow.

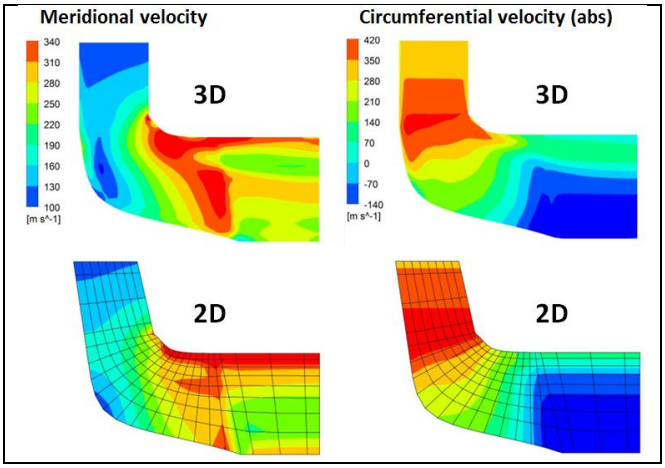

Figure 14: 2D vs. 3D CFD comparison – Low inertia

The throughflow mesh is shown on the 2D solutions to emphasise the low level of flow field discretisation. Despite this, the comparisons are considered generally good. It is apparent that the intake geometries are different. It is much easier to define the 3D intake as constant height and radial to aid prescription of the inlet flow vector. The effect on the flow field in the wheel is insignificant. The 3D meridional velocity near the trailing

edge is slightly higher than that predicted by the 2D calculation. This implies that there is some degree of aerodynamic blockage towards the trailing edge that is not modelled in the 2D simulation.

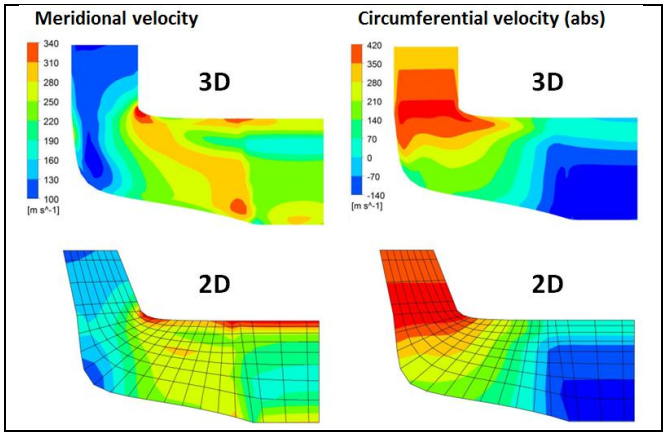

Figure 15: 2D vs. 3D CFD comparison – Mid inertia

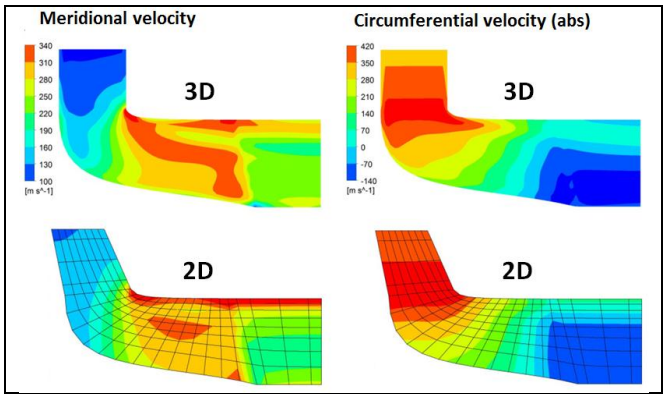

Figure 16: 2D vs. 3D CFD comparison – High inertia

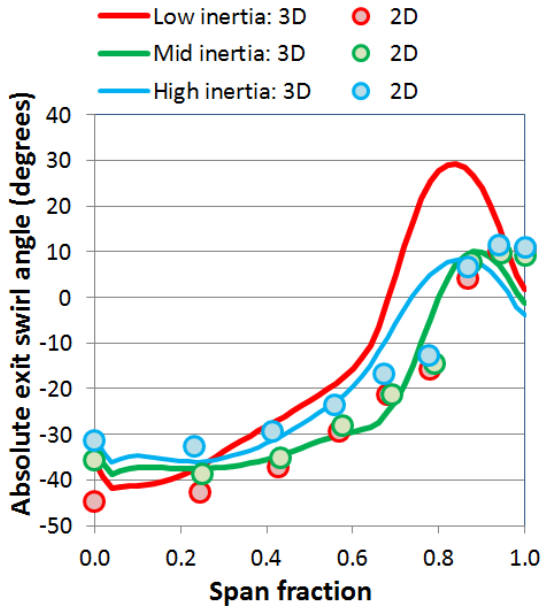

Figure 17: Exit swirl comparison – 2D vs. 3D

The only significant difference is circumferential velocity downstream of the Low inertia wheel. This must be caused by an inaccuracy in the deviation model for this case. Figure 17 compares the absolute exit swirl angle calculations. For the Mid and High inertia wheels the agreement is regarded as quite good. For the Low inertia wheel there is a significant under-turning evident in the 3D model compared to the 2D design assumption. In conjunction with the implication of a low effective throat area from Figure 13, it is concluded that there is gross suction surface separation over much of the span. This is a clear example of the limits of the 2D optimisation method. It is noted, however, that the low efficiency predicted by 3D CFD is expected based on the high optimiser aerodynamic penalty function.

5. Further development of the design

Figure 17 reveals that the mid-span exit flow from all of three of the designs has a significant swirl component. A general principle of turbine design is that the exit swirl should be close to zero to minimise the exit dynamic head. It is hoped that the optimiser has pushed the designs in this direction for a good reason, e.g. to promote strong flow acceleration in the rotor passage, but this should be tested out in 3D CFD analysis. The High inertia wheel created by the optimiser was read into ANSYS-Bladegen and the blade trailing edge angle at the hub was reduced such that the rotor throat area was increased by 7%. Note that, as a radially stacked turbine wheel it is necessary only to change the hub section blade angle. The CFD predicted performance of this wheel is plotted against the 2D optimiser wheel in Figure 18. There has been a clear change in reaction as witnessed by the increased inlet swirl angle at the design flow and the significant reduction in the absolute exit swirl angle. The design point efficiency is close to, but slightly lower than that of the optimiser design. This suggests that the optimiser has chosen correctly. The vane shape of the wheel may be refined slightly at this point to make smoother geometry.

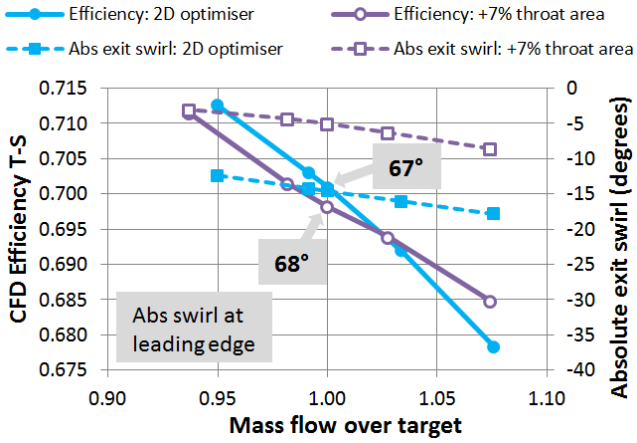

Figure 18: High inertia wheel vs. a high throat area alternative

If there are a number of potentially good designs at this stage it is useful to consider the pulse peak performance. A design that is on the Pareto front at design point conditions will usually perform at a relatively good level with pulse peak conditions, but it is worth checking all

attractive optimiser designs at both conditions. Figure 19 shows an example in which there is a design that is clearly of interest as it has the best predicted performance at both design point and pulse peak conditions.

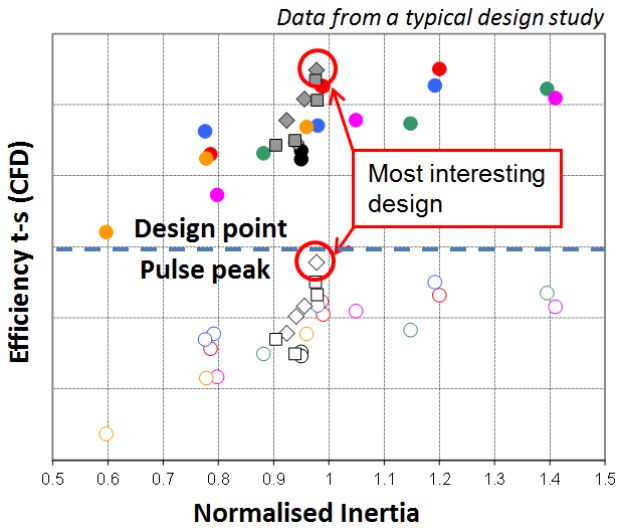

Figure 19: CFD study used to reveal the best design

5.1. Scroll design

The final aerodynamic design task is to construct a scroll for supplying the flow to the turbine wheel at the correct inlet conditions. The task is easy in principle but can be a challenge in practice especially where there is a severe constraint on diameter. The size parameter of the scroll, A/R, will be deduced approximately from the conservation of angular momentum and the inducer geometry according to:

$$\frac{A}{R} = \frac{2\pi b}{\tan \alpha_1} \qquad (2)$$

This is a constant density formulation, it ignores loss and it is difficult to assess the effective throat area, but it allows an initial scroll to be designed. It is typically designed on sections spaced at 45° from a maximum A/R set at the throat value that is then reduced linearly with azimuth angle down to the smallest practical value at 360°. The basic sizing of the scroll is confirmed using CFD in a stage calculation as shown in Figure 20 (a).

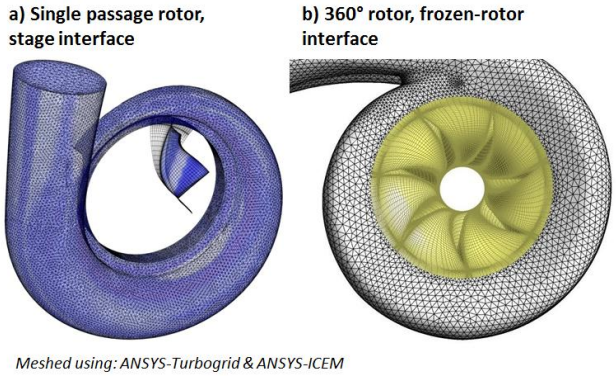

Figure 20: Full-stage calculation types

For turbocharger turbine scrolls for gasoline engines there is often the challenge of designing for a low reaction wheel. The velocity is relatively high in the scroll, which can lead to high pressure loss in the scroll, and the low passage contraction between the vanes of the wheel can lead to high sensitivity to leading edge incidence. The scroll has to be designed with great care to avoid the wheel experiencing variation in relative inlet swirl angle that is large enough to generate significant additional loss. Figure 20 (b) shows the 3D CFD model that is required for confirming acceptable flow behaviour around the full wheel. Figure 21 presents the results of a scroll design exercise where acceptably even circumferential variation has been achieved. For a good scroll design the CFD predicted efficiency from the 360° analysis should be within 1% of the single passage (stage interface) calculation. A poor circumferential distribution can lose an additional 2% or more.

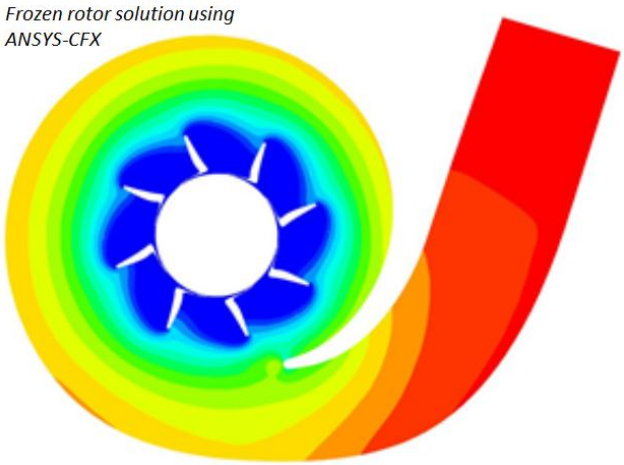

Figure 21: Static pressure field in a scroll having an optimised A/R variation

5.2. Further aerodynamic analysis

There is usually a significant difference between the efficiency calculated from main gas-path CFD, as introduced in this paper, and performance measured as that absorbed by the turbocharger compressor. The most significant reasons are usually thermal management issues and loss in the shaft bearings, which are best understood by empirical investigation on gas-stand tests. However there are subtle details of the overall gas-path geometry that can be analysed and thus improved by CFD analysis. Two examples are shown in Figure 22.

A gas-stand test, which is steady-state, will often include the exhaust manifold in the test configuration. In this case the flow to the turbine will be through one branch only. The manifold pressure loss can be calculated as a direct simulation of the test as shown in Figure 22 (a). The waste-gate port can be included too as another potential source of disturbance to the flow. Beyond this, the true transient nature of the flow can be simulated, which should include the pulses entering the manifold. This is considered to be well beyond the current topic of turbine design. A common modification to a turbine wheel,

shown in Figure 22 (b), can be considered as an extension to basic gas-path CFD based design. Significant inertia reduction is possible if the back-face of the turbine wheel is partially removed between the vanes, which is known as "scalloping". The meshing is not straightforward if the gas-path mesh is of structured form (as preferred). However, once the meshing is done, it is a relatively simple task to carry out the CFD analysis to predict the trade-off of efficiency loss and inertia reduction.

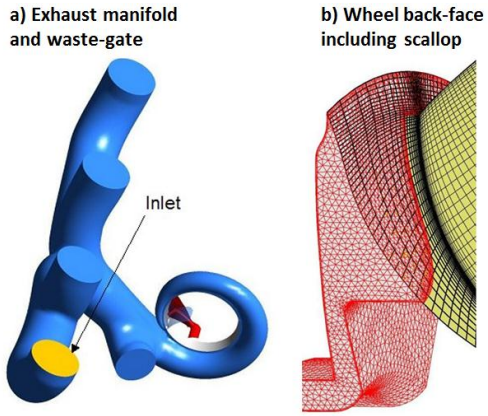

Figure 22: Areas for further aerodynamic analysis

5.3. Mechanical design

A turbocharger turbine wheel is simple in that it is a single cast component. To survive in its high temperature environment it is typically cast from a nickel-based super alloy. High cycle fatigue is not usually a problem as the only strong source of excitation is the tongue of the scroll which causes a 1/rev forcing. As noted in Table 2, the vane is usually designed to be stiff enough to have a first flap vibration frequency above 4/rev. It is advisable to carry out a forced response analysis on the wheel if the first flap frequency is much below this.

The more significant concern for the wheel is creep due to the combination of high temperature and stress. Figure 23 shows the areas likely to experience a high creep strain if the turbine undergoes excessive running at high speed and temperature.

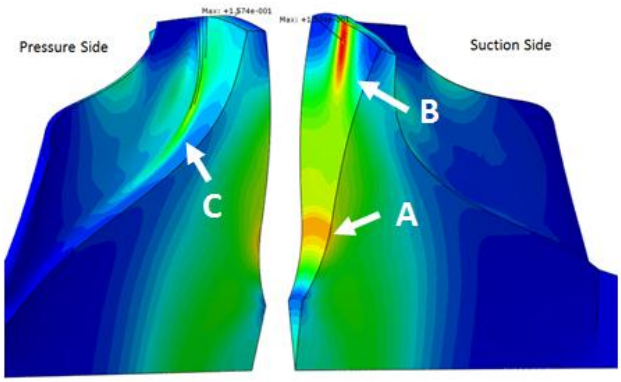

Figure 23: Creep strain in a turbine wheel

The stress at Region A, the back-face near the shaft, can be reduced to an acceptable level by making the back-face of parabolic form. The high stress at Region B is the consequence of distortion of the back-face in proximity to the vane. The underlying cause is conveniently removed by "scalloping", as mentioned in Section 5.2. This also reduces the load on the hub and will, therefore reduce the stress at Region A. The limiting feature tends to be Region C, at the vane-hub fillet at approximately mid-chord length. Careful definition of vane thickness distribution is required to make the peak stress acceptably low.

5.4. System operation

As noted at the start of Section 2 the turbine is designed to satisfy the requirements of the compressor at low engine speed where high torque is required. Low engine speed implies low turbine mass flow. The turbine stage is thus designed with a low swallowing capacity, resulting in sufficient expansion ratio to drive the compressor at its target pressure ratio.

The design low engine speed compressor ratio is identified on Figure 24 as Point 1. If sized correctly, as shown, the compressor is driven close to its surge line to maximise engine torque. If the turbine is of fixed geometry, when the engine speed increases at high load, the increasing flow through the turbine results in a high turbine expansion ratio and power output. The consequence for the compressor is that it operates at Point 2. This dramatic rise in boost pressure is experienced by the driver as an undesirable torque increase. It is also not good for the turbine life.

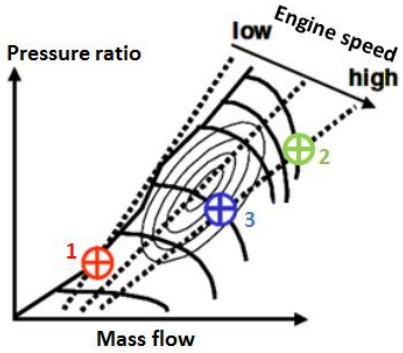

Figure 24: Operation points on the compressor map

To achieve the more desirable high engine speed boost pressure exemplified by Point 3 the swallowing capacity of the turbine must be increased as the engine flow increases. This can be achieved in an efficient manner by using a variable nozzle guide vane. Alternatively, the effect of variable swallowing capacity can be simulated by use of a turbine flow bypass (waste-gate) that results in the turbine passing a small fraction of the engine mass flow at the high engine speed condition. This results in a considerable reduction in the turbine system efficiency.

Variable nozzle guide vane systems are common in diesel engines where the engine speed range and turbine inlet temperature are relatively low. They are a challenging technology for gasoline engines mainly because of the

high temperature, but development of such systems would be of benefit for mid-flow range overall system efficiency. Figure 25 shows that the efficiency of a variable nozzle system drops off at low and high flow. It is still considered necessary to employ a waste-gate for high engine revs.

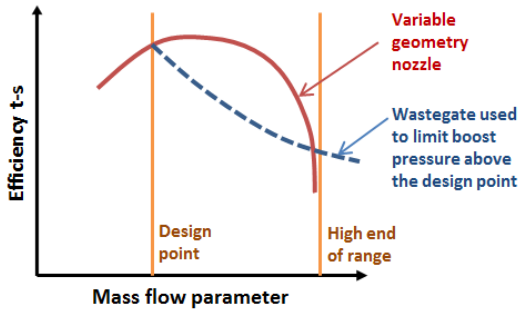

Figure 25: Turbine efficiency variation with flow for variable geometry and waste-gate systems

6. Conclusions

In this paper it has been explained that there are fairly hard constraints affecting the design of radial turbines for gasoline engines, which are mainly related to compressor design, driveability and space in the engine compartment. The major aerodynamic issues are high rotor speed and the necessity of sub-optimal diameter. Once this is accepted the task for the aerodynamic designer is to optimise a large number of geometric parameters defining the shape of the turbine wheel vane. This would be best done by assessing aerodynamic performance, within an optimisation system, using 3D CFD. Exploring the full design space using 3D CFD is still a practical challenge in the design environment so 2D CFD is proposed as a faster alternative.

It has been shown that an optimisation scheme using 2D aerodynamic analysis can produce good candidate turbine wheel designs via the production of a Pareto front of structurally acceptable designs. Comparison of 2D and 3D CFD predictions suggests that the aerodynamic performance of mid and high inertia designs can be well predicted by the 2D approach. Where the 3D flow field suffers from gross separation, as is likely for low inertia designs, the 2D agrees less well with the 3D calculation. Despite this, the aerodynamic penalty function is shown, within the small sample considered, to correlate reasonably with 3D CFD efficiency.

As shown in Figure 19, the predicted efficiency at the pulse peak condition, where a high proportion of work is extracted, correlates well with the predicted efficiency at the design point condition. It is, however, recommended that all potentially good optimiser designs should be analysed at both boundary conditions before deciding whether a design should move to the next stage of development.

For the study described it is most likely that the aerodynamic design described as “Mid inertia” would be selected for the prototype stage. It is only slightly less efficient than the design that has 70% greater inertia, and it is much more efficient that a design having 20% less inertia.

A scroll must be designed to suit the prototype turbine wheel. It should be designed with the support of 3D CFD to confirm that it will pass the correct flow and that the circumferential flow variation is acceptable for the finely optimised turbine wheel. Mechanical design issues of the wheel should be considered as soon as a vane definition is available as the thickness distribution may have to be altered to ensure acceptable creep strain over the life of the turbocharger. Finally the control of the turbine swallowing capacity must be considered to ensure the best compromise between driver experience and engine efficiency over the full speed range.

Nomenclature

b	*Inducer passage height*	mm
C	*Spouting velocity* ($=\sqrt{2\Delta h_{0S}}$)	m/s
Q	*Volumetric flow*	m^3/s
R	*Radius*	m
U	*Wheel velocity at inducer*	m/s
V	*Gas velocity (absolute)*	m/s
W	*Gas velocity (relative)*	m/s
α	*Absolute swirl angle*	°
η	*Efficiency [by default total-static, T-S]*	
ω	*Rotational speed*	rad/s
	Compound terms	
A/R	*Ratio of scroll throat area over the normal radius to the throat centroid*	mm
Δh_{0S}	*Isentropic total enthalpy drop*	J/kg
	Subscripts	
a	*Axial*	
1	*Wheel inlet*	
2	*Wheel outlet*	

Acknowledgements

The author would like to thank Michael Casey, Chris Robinson, Christian Fischer, Ian Woods and Stewart Watson for creating and developing the PCA codes used in radial turbine optimisation.

References

[1] Rohlik, H. E., Analytical determination of radial inflow turbine design geometry for maximum efficiency, *NASA Tech. Memo 4384*, 1968.

[2] Rodgers, C. and Geiser, R., Performance of a high efficiency radial/axial turbine, *Trans ASME Journal of Turbomachinery*, Volume 109, pages 151-4, 1987.

[3] Whitfield, A. and Baines, N. C., Design of radial turbomachines, *Longman Scientific & Technical, Essex*, 1990.

[4] Suhrmann, J. F., Peitsch, D., Gugau, M., Heuer, T. and Tomm, U., Validation and development of loss models for small size radial turbines, ASME GT2010-22666, *Proceedings of ASME Turbo Expo 2010*.

[5] Denton, J. D., Throughflow calculations for transonic axial flow turbines, *J. Eng. Gas Turbines Power 100(2)*, 212-218, 1978.

[6] Cox, G. D., Fischer, C., Casey, M.V., The application of throughflow optimisation to the design of radial and mixed flow turbines, *9th International conference on turbochargers and turbocharging, IMechE, London*, 2010.

[7] Cox, G. D., The practical design of turbocharger turbines using a throughflow based optimisation process, ASME GT2012-68795, *Proceedings of ASME Turbo Expo 2012*.

[8] Casey, M. V. and Robinson, C. J., A new streamline curvature throughflow code for radial turbomachinery, GT2008-50187, *Proceedings of ASME Turbo Expo 2008*.

[9] Cox, G. D., Roberts, A., Casey, M.V., The development of a deviation model for radial and mixed flow turbines in throughflow calculations, ASME GT2009-59921, *Proceedings of ASME Turbo Expo 2009*.